

# Critical properties of doped coupled spin-Peierls chains

Nicolas Laflorencie<sup>(1,2)</sup>, Didier Poilblanc<sup>1</sup>, and Manfred Sigrist<sup>3</sup>

<sup>(1)</sup> Laboratoire de Physique Théorique, Université Paul Sabatier, F-31062 Toulouse, France

<sup>(2)</sup> Department of Physics & Astronomy, University of British Columbia, Vancouver, B.C., V6T 1Z1 Canada and

<sup>(3)</sup> Institute of Theoretical Physics, ETH Hönggerberg, CH-8093 Zürich, Switzerland

(Dated: November 10, 2018)

Using numerical Real Space Renormalisation Group methods as well as Stochastic Series Expansions Quantum Monte Carlo simulations a generic model of diluted spin- $\frac{1}{2}$  impurities interacting at long distances is investigated. Such a model gives a generic description of coupled dimerized spin-Peierls chains doped with non-magnetic impurities at temperatures lower than the spin gap. A scaling regime with temperature power-law behaviors in several quantities like the uniform or staggered susceptibilities is identified and interpreted in terms of large clusters of correlated spins.

PACS numbers: 75.10.-b 71.27.+a 75.50.Ee 75.40.Mg

Low dimensional gapped quantum magnets have attracted a lot of interest in condensed matter physics for many years. The possibility of doping such systems has lead to an extremely rich emerging field. The discovery of the first non-organic spin-Peierls compound CuGeO<sub>3</sub> [1] and, soon later, its doping with static non-magnetic impurities realized by direct substitution of a small fraction of copper atoms by zinc [2] or magnesium [3] atoms offered a new challenge for the theorist and an ideal experimental system to test new theoretical concepts.

Our aim here is to analyse the low temperature properties of a typical two-dimensional array of coupled, frustrated and dimerized antiferromagnetic (AF) spin- $\frac{1}{2}$  chains doped with non-magnetic impurities. For that purpose we use the low-temperature effective model derived in previous work: each non-magnetic dopant releases a spin- $\frac{1}{2}$ , localized in its vicinity [5]. These effective spins become the only remaining low-energy degrees of freedom at temperatures lower than the spin gap i.e. the energy scale of condensation of the background spins into nearest-neighbor dimers. The corresponding effective Hamiltonian describes interacting spins  $\frac{1}{2}$  randomly distributed on a square lattice (of size  $L \times L$ ),

$$\mathcal{H}^{\text{eff}} = \sum_{\mathbf{r}_1, \mathbf{r}_2} \epsilon_{\mathbf{r}_1} \epsilon_{\mathbf{r}_2} J(\mathbf{r}_1 - \mathbf{r}_2) \mathbf{S}_{\mathbf{r}_1} \cdot \mathbf{S}_{\mathbf{r}_2}, \quad (1)$$

where the occupation number  $\epsilon_{\mathbf{r}}$  takes random values 1 (0) with probability  $x$  ( $1 - x$ ),  $x = N_s/L^2$  is the dopant concentration,  $N_s$  the number of spins  $\frac{1}{2}$ . The effective interaction  $J(\mathbf{r})$  computed by Lanczos exact diagonalizations from the original microscopic model [6] bears important properties: (i) it has opposite signs on the two (relative) sublattices and, hence, is *non-frustrating* in nature and (ii) it displays a typical (spatially anisotropic) exponential (long distance) behavior, characterized essentially by two length scales,  $\xi_{\parallel}$  and  $\xi_{\perp}$ ,

$$J(\Delta x, \Delta y) \propto -(-1)^{\Delta x + \Delta y} \exp(-\tilde{\Delta}x/\xi_{\parallel} - \Delta y/\xi_{\perp}), \quad (2)$$

where  $\tilde{\Delta}x = \Delta x + x_{\max}$  (see later) and  $\Delta x = |x_1 - x_2|$  ( $\Delta y = |y_1 - y_2|$ ) is the separation between 2 dopants in

the longitudinal (transverse) direction. Typically, we assume hereafter  $\xi_{\parallel} = 2.5$  and  $\xi_{\perp} = 1$ . Note that Eq.(2) is generic for most doped spin gapped systems [6, 7, 8]. In order to use a consistent and realistic description of the actual experimental compound, we shall use also the specific form derived in Ref. [6] at short distances for an AF interaction i.e. when  $\Delta x + \Delta y$  is odd [9]:  $J(\Delta x, \Delta y) \propto \Delta x$  up to a maximum at distance  $x_{\max} = 2\xi_{\parallel}$  ( $x_{\max} = 0$  for  $\Delta x + \Delta y$  even). At larger distances, the asymptotic form of Eq.(2) is used.

As supported by experiments [4], the present framework implies naturally that the low-temperature uniform susceptibility scales with the impurity concentration and displays a Curie-like behavior  $\chi = C/T$ . As argued in [7], due to the presence of AF as well as ferromagnetic (F) couplings [10], large (weakly coupled) clusters of spins form. Using a simple classical random walk argument, the effective spin  $S^{\text{eff}}$  of the clusters containing  $n$  spins is simply given, on average, by  $\langle S^{\text{eff}} \rangle = \frac{1}{2}\langle n \rangle^{1/2}$ . Consequently, the Curie constant (per spin) should saturate to a value equal to  $\frac{1}{3}(\langle S^{\text{eff}} \rangle)^2/\langle n \rangle = 1/12$  when  $T \rightarrow 0$ . Preliminary numerical results are in agreement with this prediction [11]. Here we shall use both numerical Real Space Renormalization Group (RSRG) [12, 13] supplemented by Stochastic Series Expansion (SSE) Quantum Monte Carlo (QMC) [14] to investigate the critical properties as one approaches the zero temperature limit.

For a single spin- $\frac{1}{2}$  chain with random AF couplings, Fisher demonstrated the existence of a universal fixed point for the renormalization group transformation [13], thus providing a strong argument in favor of such a procedure. In the case of both random F and AF couplings, while there is no exact solution, the existence of a fixed point was shown unambiguously by Westerberg et al. [10] using a RSRG approach. Its validity was discussed very carefully in [10] and the predictions were successfully checked by QMC [15]. In the similar 2D case we address here, the distribution of couplings  $P(|J|)$  behaves like  $1/|J|$  and does not depend on the dilution  $x$  (apart from logarithmic factors and a finite size cutoff  $J_{\min}$ ).

The RSRG is expected to work particularly well for such a singular distribution.

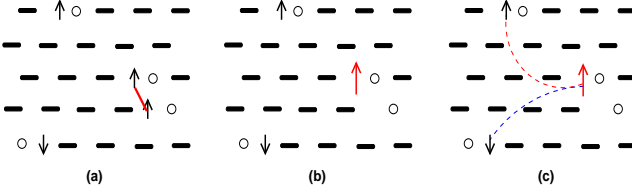


FIG. 1: Schematic picture of the doped spin-Peierls system. Thick bonds stand for dimers and non-magnetic impurities (released spins  $\frac{1}{2}$ ) are represented by open circles (black arrows). The initial RSRG step is illustrated starting from a typical configuration with 4 impurities: (a) The strongest coupled pair is identified (red line). (b) This pair, e.g. ferromagnetic here, is replaced by a spin  $S = 1$  (red arrow). (c) The couplings with all other spins (dashed lines) are renormalized.

Following the pioneering work of Bhatt and Lee [12], we extend the RSRG scheme to hamiltonian (1) with F and AF long-distance couplings [10, 16]. Let us define the effective interaction as  $J_{i,j}$  where  $i$  and  $j$  label the *randomly distributed spins* and run from 1 to  $N_s$ . One single RG step is described as follows : 1) Identify the most strongly coupled pair of spins ( $S_1, S_2$ ) i.e. with the largest energy gap  $\Delta_{1,2}$ ,  $\Delta_{1,2} = J_{1,2}(1 + |S_1 - S_2|)$  if  $J_{1,2} > 0$  (AF) and  $\Delta_{1,2} = -J_{1,2}(S_1 + S_2)$  if  $J_{1,2} < 0$  (F). Note that  $\Delta_{1,2}$  defines the energy scale of the transformation. 2) Replace it by an effective spin  $S' = |S_1 - S_2|$  if the coupling is AF or  $S' = S_1 + S_2$  in the F case. 3) Renormalize all the magnetic couplings with the following rules : (i) If  $S' \neq 0$ , as given by a first order perturbation theory, the new couplings between  $S'$  and all the other spins ( $S_3, S_4, \dots, S_{N_s}$ ) are set to

$$\tilde{J}_{(S', S_i)} = J_{1,i} c(S_1, S_2, S') + J_{2,i} c(S_2, S_1, S'), \text{ with}$$

$$c(S_1, S_2, S') = \frac{S'(S' + 1) + S_1(S_1 + 1) - S_2(S_2 + 1)}{2S'(S' + 1)}.$$

(ii) If  $S' = 0$ , the pair  $(S_1, S_2)$  is frozen. Using a cluster approximation [12] that involves only the extra pair  $(S_3, S_4)$  the most strongly coupled to  $S_1$  and  $S_2$  and a second order perturbation, the coupling  $J_{3,4}$  is renormalized as

$$\tilde{J}_{3,4} = J_{3,4} + \frac{2S_1(S_1 + 1)}{3J_{1,2}} (J_{1,3} - J_{2,3})(J_{2,4} - J_{1,4}).$$

The same procedure is then reiterated. We also check that the RSRG preserves the non-frustrated character of the problem.

Due to the presence of both F and AF couplings, clusters with large effective spins are created during the procedure similarly to what occurs in the 1D random

F-AF spin- $\frac{1}{2}$  chain [10]. At each RG step, the energy scale  $\Delta_0$  decreases and both the number of inactive spins frozen into singlets and the number of clusters build from a large number  $n$  correlated spins- $\frac{1}{2}$ , increase. The aforementioned random walk argument predicts that, the average number  $\langle n \rangle$  of spins- $\frac{1}{2}$  inside clusters and their average spin magnitude  $\langle S^{\text{eff}} \rangle$  should be related by  $\langle S^{\text{eff}} \rangle \sim \langle n \rangle^{1/2}$  at low enough temperatures. Therefore we expect the effective spin of these clusters to grow monotonously as the energy scales down. We have analyzed this process using the RSRG scheme to compute both  $\langle S^{\text{eff}} \rangle$  and  $\langle n \rangle$  as a function of  $\langle \Delta_0 \rangle$ . This is shown in Fig. 2 which clearly demonstrates the formation of large moments. Moreover, power-law divergences like  $\langle S^{\text{eff}} \rangle \sim \langle \Delta_0 \rangle^{-\alpha(x)}$  and  $\langle n \rangle \sim \langle \Delta_0 \rangle^{-\kappa(x)}$  are observed with  $\kappa \simeq 2\alpha$ . We have plotted the behavior of these exponents vs  $x$  in Fig. 7. Interestingly enough, we find that  $\alpha$  depends on  $x$  in contrast to the random F-AF spin chain for which  $\alpha = 0.22 \pm 0.01$  [10]. Note however that the universality class identified in [10] as a RG fixed point occurs only for initial gap distributions less singular than  $P_c(\Delta) \sim \Delta^{-y_c}$ , with  $0.65 \lesssim y_c \lesssim 0.75$ . For more singular distributions, as it is the case here, critical exponents are not universal anymore, at least in 1D [10].

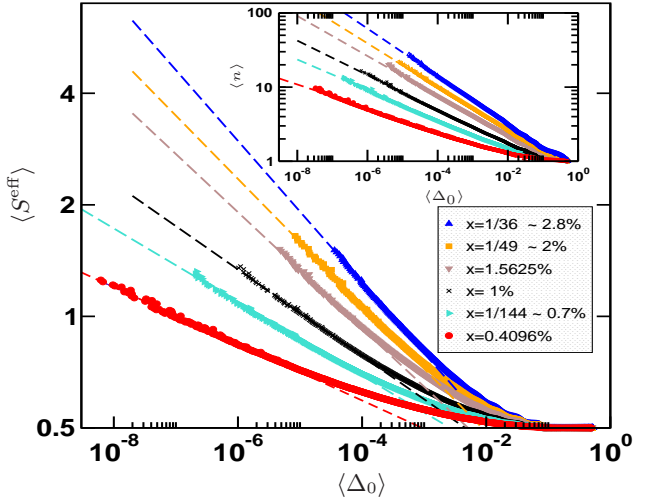


FIG. 2: Average effective spin  $\langle S^{\text{eff}} \rangle$  of the clusters of active spins vs the energy scale  $\langle \Delta_0 \rangle$  for six different concentrations  $x$  indicated on the plot. Numerical RSRG data obtained for  $N_s = 1024$  spins over more than  $10^4$  samples. Inset: for the same samples, average number  $\langle n \rangle$  of initial spins- $\frac{1}{2}$  per cluster vs  $\langle \Delta_0 \rangle$ . Dashed lines are power-law fits (see text).

We now turn to a brief discussion about the validity of the RSRG approach w.r.t. the large (formally infinite) connectivity of the model. Whereas the moments eventually order AF at zero temperature for arbitrary small concentration [11], at finite temperatures the physics is dominated by short range couplings, i.e. inside a domain defined by  $\Delta x \leq \xi_{\parallel}$  and  $\Delta y \leq \xi_{\perp}$ . Consequently, one could

define a "short-range connectivity number"  $z_{sr}$  which is, for a given spin, the average number of neighboring spins belonging to such a short range couplings region. It is easy to check that  $z_{sr} = \mathcal{N}_{sr}x(1 - N_s^{-1}) \simeq \mathcal{N}_{sr}x$  where  $\mathcal{N}_{sr}$  is the number of sites contained in the short-range region. For the present model  $\mathcal{N}_{sr} \simeq 65$  sites as seen numerically. The evolution under the RSRG scheme depends on the value of  $z_{sr}$ , hence on  $x$ . When, let us say,  $z_{sr} < 1$  (i.e.  $x < 1.55\%$ ), the probability to have extra spins strongly coupled to the most strongly coupled pair ( $S_1, S_2$ ) remains very small, so that the necessary condition  $J_{1,2} \gg J_{1,i}, J_{2,i}, \forall i > 2$  is fulfilled. On the other hand, if  $z_{sr} > 2$  (i.e.  $x > 3.1\%$ ) a "percolation threshold" is reached and one expects the formation of strongly coupled clusters reaching the system size.

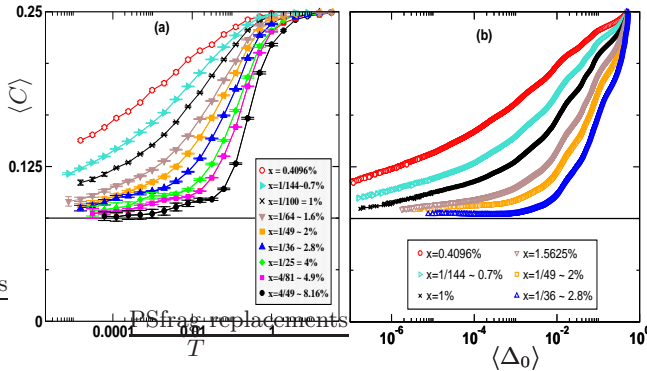


FIG. 3: Curie constant per spin  $\langle C \rangle$  plotted vs the energy scale. (a) Quantum Monte Carlo SSE results shown vs  $T$  for  $N_s = 256$  spins and 9 different concentrations  $x$  indicated on the plot. Disorder is performed on  $10^3$  to  $10^4$  samples. (b) Numerical RSRG results shown for  $N_s = 1024$  spins and 6 different concentrations  $x$  as indicated on the plot, vs the RG energy scale  $\langle \Delta_0 \rangle$ . Error bars are typically smaller than symbol sizes, the number of samples always exceeding  $10^4$ . The full line correspond to the saturation value of  $1/12$ .

Since the above arguments are still qualitative [17], we have confronted the RSRG results to QMC data obtained on the same model and for the same parameters. The SSE method [14] supplemented by the  $\beta$ -doubling scheme [18], already used in [11], can reach extremely low temperatures. Figs. 3 show results for the Curie constant per spin obtained with both methods. The RSRG computation of  $C$  is performed, at each RG step, using the formula  $C = \frac{1}{3N_s} \sum_{\sigma} N_{\sigma} \sigma(\sigma + 1)$  where  $N_{\sigma}$  is the number of active effective spins of size  $\sigma$ , the data being then averaged over disorder. We have also checked that finite size effects are negligible when  $N_s \geq 256$  and we have chosen  $N_s = 1024$  in most computations. We observe a qualitative agreement between Fig.3(a) and Fig.3(b) where, at high temperatures, the spins behave as paramagnetic free magnetic moments (giving a Curie constant of  $\frac{1}{4}$  per spin) and where saturation to  $\frac{1}{12}$  is observed at low  $T$ , the spins being correlated inside large clusters. At

small concentration, the agreement becomes even quantitative, as seen in the Fig.4 where a comparison between RSRG and SSE is shown for the six lowest values of  $x$ . The agreement remains quite good for larger concentra-

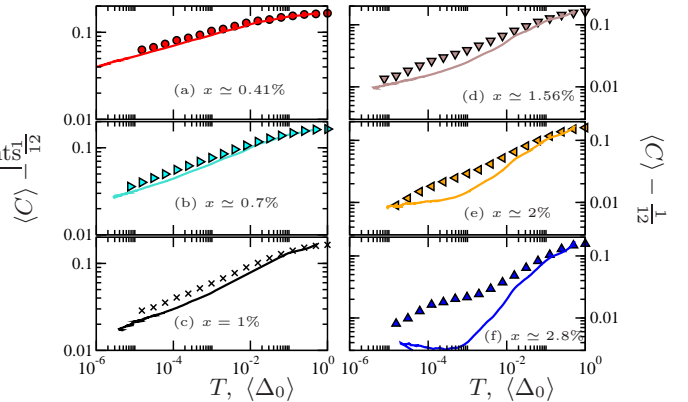


FIG. 4: Direct comparisons between RSRG (full lines) and SSE simulations (symbols) of  $\langle C \rangle - 1/12$  are shown for the 6 different concentrations indicated by (a), (b), ..., (f) vs the RG energy scale  $\langle \Delta_0 \rangle$  or the SSE temperature  $T$ .

tion up to  $x \simeq 1.56\%$  corresponding to  $z_{sr} \simeq 1$ , hence corroborating the qualitative argument stated above.

We now turn to the analysis of the scaling regime. At very low temperatures, the quantum corrections  $\langle C(T) \rangle - 1/12$  are expected to behave like  $T^{\gamma}$  where  $\gamma = \alpha$  in 1D [15]. In the present case, the procedure used in Figs. 5

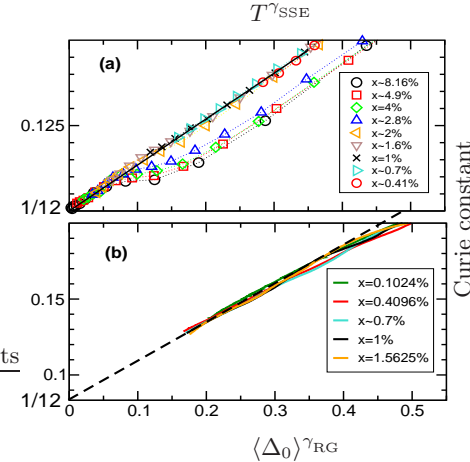


FIG. 5: Curie constant  $\langle C \rangle$  plotted vs  $T^{\gamma_{SSE}}$  for the QMC data in (a) and vs  $\langle \Delta_0 \rangle^{\gamma_{RG}}$  for the RSRG data in (b), in order to obtain the best data collapse at low energy.

to extract the doping dependence of  $\gamma$  from the QMC and RSRG susceptibility data is the following: First, one estimates the value of  $\gamma$  at the lowest concentration available, i.e.  $x_{\min} \simeq 0.41\%$  for the SSE and  $x_{\min} = 0.1\%$  for the RG, via a direct reliable power-law fit, giving  $\gamma_{SSE} = 0.12$

and  $\gamma_{RG} = 0.065$  in those cases. Then, the other estimates for larger  $x$  are determined in order to obtain the best collapse of all the data plotted vs  $T^\gamma$  on a universal low temperature curve, as shown in Figs. 5. We note that, for large  $x$ , deviations at high temperatures can be attributed to a transient and plateau regimes also visible in Fig. 3(a) for  $x \geq 1/36$  [20]. Similarly, one expects for the

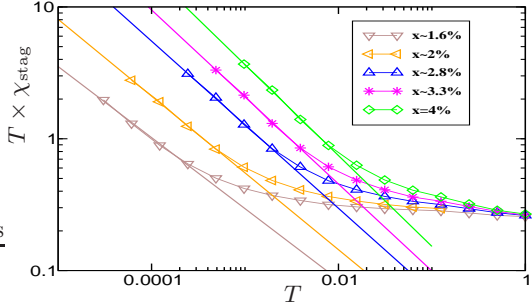


FIG. 6:  $T\langle\chi_{\text{stag}}(T)\rangle$  plotted vs  $T$  for five different concentrations. Full lines are fits corresponding to power-law behaviors  $\sim T^{-2\gamma'}$ . All data are computed by QMC using  $N_s = 256$  random spins and averaged over disorder.

staggered susceptibility (per spin),  $\langle\chi_{\text{stag}}(T)\rangle \propto T^{-1-2\gamma'}$ . In 1D,  $\gamma'$  is expected to be equal to  $\alpha$  [19], but in the present case, by direct fits of the low  $T$  (see Fig. 6), we found  $\gamma' \simeq \gamma \simeq 2\alpha$ . Those exponents are plotted

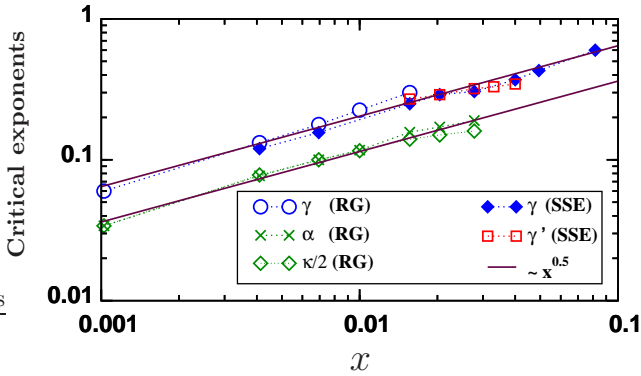


FIG. 7: Exponents  $\alpha(x)$ ,  $\gamma(x)$  and  $\gamma'(x)$  extracted from various SSE and RSRG data as indicated on the plot (see text for details). Straight lines are  $\sim \sqrt{x}$ .

in Fig. 7. An overall very good agreement is seen between the different methods, in particular between the estimates of  $\gamma$  obtained from the analysis of the Curie constant computed by QMC and RSRG. We stress again that the exponent  $\alpha$  deduced from the analysis of the change of cluster sizes and spins is roughly a factor of 2 smaller than  $\gamma$ . Interestingly enough,  $\gamma \simeq 2\alpha \propto \sqrt{x}$  in all cases.

To conclude, confronting results obtained by both state-of-the-art QMC simulations and numerical RSRG

methods, we have achieved a physical understanding of the critical properties of a generic 2D model of diluted  $S = \frac{1}{2}$  spins with long-ranged interactions. For small dopant concentration, the RSRG appears to be in excellent agreement with QMC computations. Power-law temperature behaviors in several quantities like the uniform or staggered susceptibilities are revealed and interpreted in terms of large clusters of correlated spins which also have interesting scaling properties with temperature. It is remarkable that such properties are observed above the  $T = 0$  ordered magnetic groundstate. Moreover, it is the first example of a two-dimensionnal random magnet exhibiting a large spin phase with a disorder (the concentration  $x$ ) dependence of the critical exponents. Whereas doped CuGeO<sub>3</sub> might be a good candidate for the experimental observation of a critical regime, the so large three-dimensionnal ordering temperature prevents such an observation. More strongly diluted samples are necessary to reach the scaling regime.

*Acknowledgment:* We are indebted to A.W. Sandvik for providing some QMC codes and for valubles comments. DP also thanks T. Giamarchi for usefull discussions.

---

- [1] M. Hase, I. Terasaki, and K. Uchinokura, Phys. Rev. Lett. **70**, 3651 (1993).
- [2] M. Hase, I. Terasaki, Y. Sasago, K. Uchinokura, and H. Obara, Phys. Rev. Lett. **71**, 4059 (1993).
- [3] S.B. Oseroff *et al.*, Phys. Rev. Lett. **74**, 1450 (1995); L.-P. Regnault *et al.*, Europhys. Lett. **32** 579 (1995); T. Masuda *et al.*, Phys. Rev. Lett. **80**, 4566 (1998).
- [4] B. Grenier *et al.*, Phys. Rev. B **58**, 8202 (1998).
- [5] E. Sorensen *et al.*, Phys. Rev. B **58**, R14704 (1998).
- [6] N. Laflorencie and D. Poilblanc, Phys. Rev. Lett. **90**, 157202 (2003).
- [7] M. Sigrist and A. Furusaki, J. Phys. Soc. Japan **65**, 2385 (1996).
- [8] S. Wessel *et al.*, Phys. Rev. Lett. **86**, 1086 (2001).
- [9] This originates from the location of the moments on *opposite* sides of the two dopants. Note also that, *on the same chain*, the AF interaction decreases linearly to  $\simeq 0$  at a rather long distance  $\xi_{\parallel}^0 \simeq 17$ ; see Ref. [6].
- [10] E. Westerberg *et al.*, Phys. Rev. Lett. **75**, 4302 (1995); A. Furusaki *et al.*, Phys. Rev. B **52**, 15930 (1995); E. Westerberg *et al.*, Phys. Rev. B **55**, 12578 (1997).
- [11] N. Laflorencie *et al.*, Phys. Rev. B **69**, 212412 (2004).
- [12] R. N. Bhatt and P. A. Lee, Phys. Rev. Lett. **48**, 344 (1982).
- [13] D. S. Fisher, Phys. Rev. B **50**, 3799 (1994).
- [14] A. W. Sandvik, Phys. Rev. B **59**, R14157 (1999); A. W. Sandvik, Phys. Rev. E **68**, 056701 (2003).
- [15] B. Frischmuth and M. Sigrist, Phys. Rev. Lett. **79**, 147 (1997); B. Frischmuth *et al.*, Phys. Rev. B **60**, 3388 (1999).
- [16] R. Mélin, Eur. Phys. J. B **16**, 261 (2000); Y.-C. Lin *et al.*, Phys. Rev. B **68**, 024424 (2003).
- [17] We have also computed the mean gap  $\langle\Delta\rangle$  and checked

that the ratio  $\langle \Delta \rangle / \langle \Delta_0 \rangle$  remains  $\leq 10^{-2}$ .

- [18] A. W. Sandvik, Phys. Rev. B **66**, 024418 (2002).
- [19] N. Nagaosa *et al.*, J. Phys. Soc. Japan **65**, 3724 (1996).
- [20] Such a behavior can be understood as an effective “en-

ergy gap” in the distribution of effective couplings, due a short-range connectivity number larger than 1.